



# On wetting behavior of fluorocarbon coatings with various chemical and roughness characteristics

S.A. Kulinich<sup>\*</sup>, M. Farzaneh<sup>1</sup>

*Canada Research Chair on Atmospheric Icing Engineering of Power Networks and Industrial Chair on Atmospheric Icing of Power Network Equipment, Université du Québec à Chicoutimi, Canada G7H 2B1*

Received 4 February 2005; received in revised form 19 April 2005; accepted 21 April 2005

## Abstract

This study aims at analyzing the hydrophobicity of a wide range of fluorine–carbon coatings, from carbon-rich to fluorine-rich materials, carried out within the framework of a search for snow- and ice-repellent materials. A simple model accounting for both surface chemical composition and roughness was applied to evaluate the wettability of various fluorocarbon coatings. Apparent contact angles of water on both smooth and rough surfaces are modeled as functions of the fluorination degree and area fraction of air entrapped into the water–solid interface. It is shown that low-fluorinated C–F coatings are hardly hydrophobic and likely will not provide snow or ice-repellent properties. At the same time, coatings with higher F concentration demonstrate good hydrophobicity, which can be further enhanced by air entrapment into rough surface structures. Thus, as coatings with good mechanical properties, low surface energy and surface roughness governed by deposition parameters, such C–F materials may be of potential use for snow- and ice-repellent purposes.

© 2005 Elsevier Ltd. All rights reserved.

PACS: 68.35.M; 68.45.G

*Keywords:* Fluorocarbon coatings; Low surface energy; Water repellency; Surface roughness; Snow repellency; Ice repellency

## 1. Introduction

Various amorphous carbon coatings are well known for their high hardness, wear resistance,

chemical inertness, and low friction coefficients [1–6]. Their properties may be further modified by incorporating various doping species, such as metals, nitrogen, oxygen, and silicon [1,3–5,7–14]. The fluorine incorporation into diamond-like carbon (DLC) coatings has been reported to considerably reduce their surface free energy [1,4,11–13]. Also, the hardness and Young's

<sup>\*</sup>Corresponding author. Fax: +1 418 545 5032.

E-mail address: [s\\_kulinich@yahoo.com](mailto:s_kulinich@yahoo.com) (S.A. Kulinich).

<sup>1</sup>Chairholder (CIGELE/INGIVRE).

modulus of such films, as well as their surface energy, decrease at high F content [1,5,12–14], and films tend to become more graphitized and polymer-like [1,5,12,15–18].

A wide variety of fluorinated carbon films, from relatively hard to fairly soft (or polymer-like), have been produced by plasma-enhanced CVD (PECVD) from fluorocarbon–hydrocarbon precursors [1,4,7,11–14], RF glow discharges fed with tetrafluoroethylene [19], sputtering of polytetrafluoroethylene (PTFE) [5,16,17], or post-deposition  $\text{CF}_4$  treatment of carbon films [11]. The films had high water contact angles of  $\sim 80$ – $170^\circ$  depending on process parameters and precursors used [1,11,12,16,19–21].

In cold regions, there is always a critical problem of decreasing the adhesion of snow and ice to structures under low-temperature conditions. In recent years, various water-repellent coatings have been proposed for this purpose. Saito et al. [22] have reported the preparation of highly water-repellent coatings based on PTFE particles dispersed in polyvinylidene fluoride resin binder and their ice-repellent properties. It was shown that the free surface energy of the coatings has a linear relationship with the adhesion of ice. Somlo and Gupta [23] also showed decrease in ice adhesion on surfaces with lower surface energy. Kako et al. [24] have demonstrated reduced wet-snow adhesion on a superhydrophobic surface compared to that on a hydrophobic one.

Ji et al. [12,13] have first proposed fluorinated carbon coatings for snow- and ice-repellent applications. They deposited fluorinated DLCs on silicate glaze and aluminum substrates as potentially hydrophobic and ice-phobic coatings for both insulators and conductors for electrical utilities in power lines, and evaluated their hydrophobicity. More recently, Futama et al. [25] have also proposed thermally sprayed fluorine–carbon coatings for snow-repellent applications, which after modification by silinization reached contact angles around  $130^\circ$ .

In their works, Petrenko and Peng [26] and Saito et al. [22] reported linear correlation between hydrophobicity of certain materials and their ice repellency. As wetting, in most cases, is the first stage of icing or wet-snow adhesion events, wetting

behavior of a-C:F coatings, as potential snow- or ice-repellent materials, should be first evaluated. Hence, hydrophobicity of fluorocarbon coatings with various degrees of fluorination and roughness is theoretically considered in this work based on the theoretical approach, which was previously applied by us to surfaces coated with alkylsilane self-assembling monolayers [27,28].

## 2. Model description

According to the two major models describing fluorocarbon film structure, F-rich films are polymer-like with C–C chains,  $\text{CF}_2$  units, and small amounts of cross-linking C–C units [1,5,13,14]. At the same time, fluorocarbons with low F concentrations are of DLC structure with irregular carbon circles [5]. Therefore, a model to evaluate the wetting behavior of various C–F coatings, from harder fluorinated DLC films (low F content) to softer polymer-like coatings (high F content) is proposed with the following assumptions.

We assume C–F coatings are heterogeneous and composed of two phases, which have a uniform distribution over the surface. The first phase is the “teflon-like” one, and this assumption is based on the fact that fluorocarbon ( $\text{CF}_x$ ) coatings with  $x$  very close to that of Teflon ( $x = 2$ ) have been achieved [17,18]. The other phase is the “carbon-like” one. The wettability of a smooth  $\text{CF}_x$  surface is defined by relative contribution of the two above phases, with domains of molecular-size dimension, which interplay with water.

For simplicity, the “fluorinated-carbon” domains are assumed to have a contact angle with water equal to that of Teflon ( $\theta = 108^\circ$ ) [6,27], although generally, fluorinated carbon coatings may include various  $\text{CF}_n$  groups with  $n = 1$ – $3$  [5,11,12]. Also, for simplicity, the “pure-carbon” domains are ascribed to have a contact angle of  $80^\circ$ . The choice of this value is based on the following experimental data reported in the literature for smooth coatings:  $\theta = 82.3^\circ$  for PECVD-deposited DLC [7] and  $\theta = 75.6$ – $80.3^\circ$  for various amorphous carbon coatings made by filtered cathodic vacuum arc [2,8,10]. Note that

the contact angle on graphite was reported to be of  $85.7^\circ$  [29], which is also somewhat below  $90^\circ$ .

The area fractions of the two phases are described by the parameters  $f_t$  and  $f_c$ , with their sum being  $f_t + f_c = 1$ . Highly fluorinated surfaces, similar to those reported in [17,18], are described by  $f_t$  close to 1. Rough surfaces and air inclusion in the surface structure are modeled by changing surface area fractions of water- and air-covered “teflon-like” and “carbon-like” domains.

According to Israelachvili and Gee [30], the contact angle of water droplet on chemically inhomogeneous and smooth surface with nano-sized domains of “teflon-like” and “carbon-like” phases can be expressed by Eq. (1):

$$(1 + \cos \theta)^2 = f_t(1 + \cos \theta_t)^2 + f_c(1 + \cos \theta_c)^2, \quad (1)$$

where  $\theta$  is the contact angle on a flat inhomogeneous surface consisting of two phases with nano-sized patches;  $\theta_t$  and  $\theta_c$  are contact angles on pure materials;  $f_t$  and  $f_c$  are fractional areas of the materials ( $f_t + f_c = 1$ ).

When a solid surface is rough, Eq. (1) is modified into the Wenzel Eq. (2) to describe the contact angle  $\theta_r$  on a rough surface by considering the increase in the actual surface area [31,32]:

$$\cos \theta_r = r \cos \theta. \quad (2)$$

Here,  $r$  is the roughness factor, i.e., the ratio of the actual area of a rough surface to the geometric projected area.

When the roughness factor of a hydrophobic surface is above a certain value, the system enters the Cassie wetting regime, in which water does not penetrate into the troughs (see Fig. 1a) [20,32,33]. Such surfaces are referred to as “composite” because the intersection of the water droplet with the surface consists of a composite mixture of water–air and water–solid interface area. The wettability of such surfaces is expressed by Eq. (3) [27,28,32,33]:

$$\cos \theta^c = f^w \cos \theta - f^a, \quad (3)$$

where  $\theta^c$  is the contact angle of water on a “composite” surface with air entrapped;  $f^w$  and  $f^a$  are the area fractions of the water- and air-covered solid surface, respectively ( $f^w + f^a = 1$ ). Eq. (3)

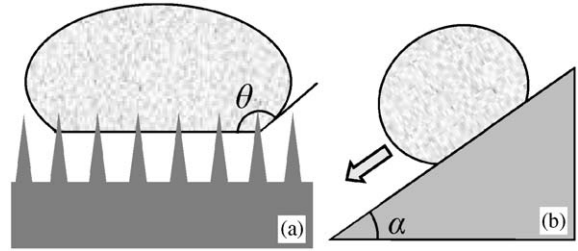


Fig. 1. (a) Water droplet on hydrophobic surface with needle-like structure; air is entrapped between the droplet and surface. (b) Water droplet starts sliding on inclined hydrophobic surface. Contact angle ( $\theta$ ) and sliding angle ( $\alpha$ ) are shown.

describes wetting of a homogeneous “composite” surface.

A procedure to modify Eq. (3), in order to describe contact angles of water droplets on two-phase chemically inhomogeneous “composite” surfaces, can be found in [27,28]. Omitting the derivation procedure, which introduces air pockets between a two-phase chemically heterogeneous solid surface and water droplet, we arrive at Eq. (4). This equation describes the equilibrium contact angle of water on rough chemically heterogeneous surfaces of two phases (formed by fluorinated and “carbon-like” phases) with air trapped:

$$\cos \theta^* = f_t(f_t^w(1 + \cos \theta_t) - 1) + (1 - f_t)(f_c^w(1 + \cos \theta_c) - 1), \quad (4)$$

where  $\theta^*$  is the contact angle on a “composite” fluorocarbon surface;  $f_t^w$  is a fractional surface area of water-covered “teflon-like” phase; and  $f_c^w$  is a fractional surface area of water-covered “carbon-like” phase.

While the contact angle of water has been commonly used as a criterion for the evaluation of surface hydrophobicity, this alone is insufficient for the evaluation of the sliding properties of water droplets on surfaces [33–37]. A surface with a high contact angle does not always show a low sliding angle, which is defined as the critical angle where a water droplet with a certain weight begins to slide down the inclined substrate. Moreover, very recently, sliding behavior has been used as a measure of wet-snow repellency of surfaces [24].

Therefore, where hydrophobicity is concerned, the sliding angle of water droplet (at which the latter starts sliding on inclined surfaces, Fig. 1b) should be evaluated separately from the contact angle [33,35–37]. To qualitatively evaluate sliding angles of rough “composite” fluorocarbon coatings, we adopt Eq. (5), which was derived by Miwa et al. [33] to describe sliding angles of water droplets on rough hydrophobic surfaces with needle-like posts. Fig. 1a presents an example of such a surface. In many cases, fluorocarbon coatings can be produced with their surface posts having pyramid- or cone-like tops with the  $R$  parameter slightly over 1 [20,21]; and it is believed that for such structures Eq. (5) can be applied.

$$\sin \alpha = \frac{2Rk \sin \theta^* (\cos \theta^* + 1)}{g(R \cos \theta + 1)} \times \left( \frac{3\pi^2}{m^2 \rho (2 - 3 \cos \theta^* + \cos^3 \theta^*)} \right)^{1/3} \quad (5)$$

Here  $\alpha$  is the minimum angle of surface tilt at which a droplet will spontaneously move;  $R$  is the ratio of the side area to the projected area of the needle-like post;  $\theta$  and  $\theta^*$  are contact angles on flat and rough surfaces (determined from Eqs. (1) and (4)), respectively;  $m$  and  $\rho$  are the mass and specific weight of the liquid droplet, respectively;  $g$  is the acceleration of gravity; and  $k$  is a constant with a dimension of  $\text{mJ}/\text{m}^2$ , which was related by Murase and Fujibayashi to the interaction energy between solid and liquid [35].

### 3. Results and discussion

#### 3.1. Effect of fluorination degree and roughness

Fig. 2 shows the influence of the fluorination degree of smooth (curve 1) and rough in the Wenzel regime (curves 2 and 3) coatings on the contact angle of a sessile water droplet, as calculated from Eqs. (1) and (2) in the Wenzel wetting regime. Whereas the maximum achieved on flat surfaces equals  $108^\circ$ , corresponding to the coating of pure Teflon, on roughened surfaces increased values can be expected (curves 2 and 3). It is also seen that on both flat and rough surfaces,

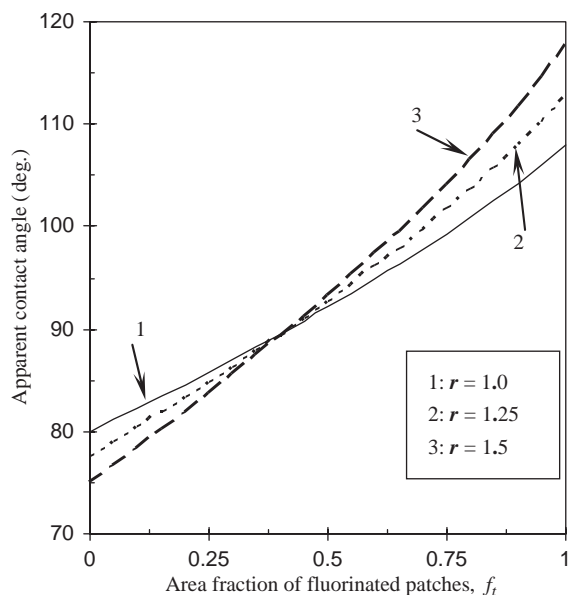


Fig. 2. Contact angle of fluorinated carbon coatings as a function of fluorination degree calculated from Eqs. (1) and (2). Effect of surface roughness in Wenzel's wetting regime is also shown for surfaces with the roughness factor  $r = 1.0$  (1), 1.25 (2), and 1.5 (3).

the contact angle of water increases as the fluorination degree increases and coatings tend to be more “teflon-like”.

Another important observation is that below some certain value of the fluorination degree (which corresponds to  $\theta = 90^\circ$  on flat surface) coatings become more hydrophilic with increase in roughness in the Wenzel regime (see curves 2 and 3 at  $f_i \sim 0.4$  and below). Such surfaces, when their roughness is further increased, cannot trap air in their troughs and, therefore, are not considered in the next sections in which we deal with “composite” surfaces with air inclusions.

It should be mentioned that surface roughness of various fluorocarbon coatings can be increased by using appropriate deposition parameters, for instance, higher pressure of feedstock gas [12], higher pressure of ambient Ar while sputtering PTFE [16], or using modulated plasma [19]. Another approach is to use patterned substrates [3,9,20] or pre-sputtered CrN underlayers with different surface features created before C–F coatings [21].

### 3.2. Effect of air inclusion in rough surfaces

Because of the uniform surface distribution of fluorinated and “carbon-like” domains, and based on the assumption of air inclusions at micrometer scale or over, it can be expected that on real rough fluorocarbon coatings with air entrapped, the condition of  $f_t^w \sim f_c^w$  will be realized. Therefore, hereafter hydrophobicity on “composite” surfaces will be evaluated mainly under the condition of  $f_t^w = f_c^w$ . Also, as mentioned earlier, we do not consider fluorination degrees  $\sim f_t < 0.5$ , as “composite” surfaces are hardly expected at low  $F$  content.

The importance of air inclusion into surface structures for achieving high water contact angles has been emphasized by a number of researchers [20–22,32,33]. Fig. 3a and b shows the relations between  $\theta^*$  and  $f_t$  and  $f_t^w$ , as calculated from Eq. (4) for “composite” fluorocarbon surfaces in the Cassie wetting regime. Two different cases of water coverage of “carbon-like” patches with  $f_c^w = 0.25$  (a) 0.75 (b) are presented. It can be seen that higher values of  $\theta^*$  are attained when  $f_t^w$  and  $f_c^w$  are lower, and the fluorination degree is enhanced ( $f_t$  close to 1). When water-coverage fraction of the “carbon-like” phase is increased (Fig. 3b), the contact angle  $\theta^*$  decreases. However, its tendency,

with respect to  $f_t$  and  $f_t^w$ , remains the same as for lower values of  $f_c^w$  (Fig. 3a).

The same tendencies are observed in Fig. 4a, where the relation between  $\theta^*$  and  $f_t^w$  and  $f_c^w$  is shown for the coatings with a fluorination degree of  $f_t = 0.5$ . Again, lower water coverage of both fluorinated ( $f_t^w$ ) and “carbon-like” ( $f_c^w$ ) phases lead to higher values of equilibrium contact angle  $\theta^*$ . It is also seen in Figs. 3 and 4a that contact angles of water much higher than  $120^\circ$  (maximum possible for a smooth  $\text{CF}_3$ -terminated surface) can be achieved on rough surfaces under certain conditions.

Fig. 4b compares contact angles on “composite” fluorocarbon surfaces with different fluorination degrees as a function of water-coverage fraction  $f_t^w = f_c^w$ . It is clear that water repellency of the coatings is enhanced with reduced water coverage of the solid surfaces ( $f_t^w = f_c^w$ ) and increased  $F$  content ( $f_t = 0.5, 0.7, \text{ and } 0.9$  for curves 1, 2, and 3, respectively). The results in Fig. 4b are in reasonable agreement with the experiment of Cheng et al. [20] who measured contact angles on Ag nanowires coated with PECVD-deposited fluorocarbon films. Based on the value of  $155^\circ$  and assuming the coating’s composition within those described by curves 1–3 in Fig. 4b, one can conclude that water coverage of the sample was

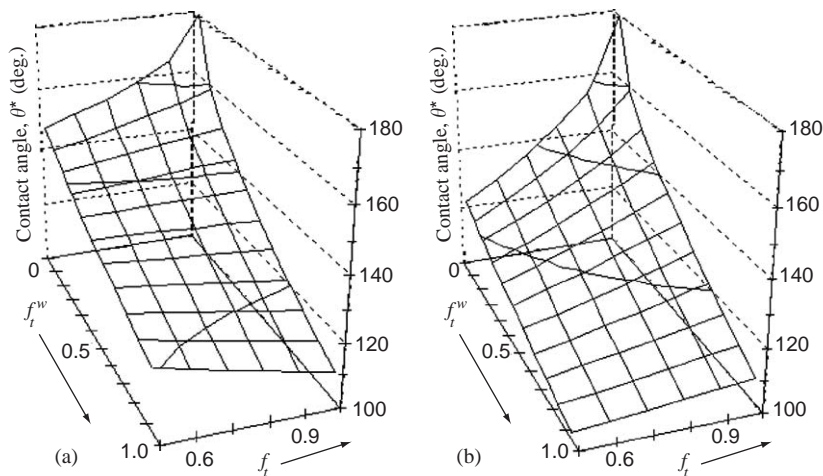


Fig. 3. Contact angle of “composite” fluorocarbon surfaces as a function of fluorination degree ( $f_t$ ) and water coverage of fluorinated patches ( $f_t^w$ ) calculated from Eq. (4) in the Cassie wetting regime. The water coverage of “carbon-like” patches ( $f_c^w$ ) equals 0.25 (a) and 0.75 (b). Only coatings with  $f_t \geq 0.5$  are considered.

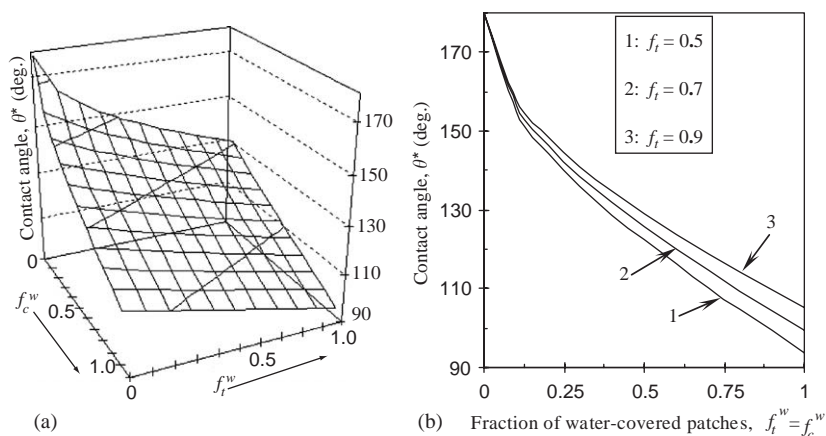


Fig. 4. (a) Contact angle of “composite” fluorocarbon surfaces calculated from Eq. (4) in the Cassie wetting regime as a function of water coverage of “teflon-like” patches ( $f_t^w$ ) and “carbon-like” patches ( $f_c^w$ ) at fluorination degree  $f_t = 0.5$ . (b) Contact angle as a function of area fraction of surface water-covered patches ( $f_t^w = f_c^w$ ) for surfaces with different fluorination degree:  $f_t = 0.5$  (1), 0.7 (2), and 0.9 (3).

~10–12%. This value is lower than the total area of nanowires’ tops, but somewhat different nanowires’ height and nanoscale roughness of their tops should be considered, too. At the same time, Fig. 4b predicts that the C–F ribbon-shaped structures with F:C = 1.68 deposited from  $C_2F_2$  by modulated r.f. plasma [19] had water coverage of a few % only, as they demonstrated contact angles as high as  $170^\circ$ .

It should also be mentioned that the condition of  $f_t^w = f_c^w$  for various fluorocarbon coatings in Fig. 4b implies their equal water-coverage fractions, rather than equal geometrical surface topologies. We suppose that the lower-fluorinated surfaces (curve 1) in Fig. 4b should have more “advantageous” topographies compared to those with higher F content (curves 2 and 3) to satisfy the same requirement of  $f_t^w = f_c^w$ , as being higher-energy surfaces. For this reason, it is believed that on substrates with the same topographies, a difference somewhat greater than that between the curves in Fig. 4b should be expected, since a higher water-coverage regime for low-F-content coatings should be realized (with deeper water penetration into surface troughs).

The results presented are supported by the experimental results reported by Favia et al. [19] for their highly hydrophobic coatings prepared from tetrafluorethylene in modulated RF glow

discharge. Combined high fluorination degree and surface texture/roughness led to the super-hydrophobic behavior of surface with water contact angles up to  $170^\circ$  [19]. Ji et al. [12,13] also reported that the wettability of their PECVD-fabricated  $CF_x$  films from  $C_3F_8$  precursor could be controlled by two factors: the fluorine content and surface morphology. The apparent contact angles of water thus attained were up to  $130^\circ$  [12,13].

### 3.3. Dynamic hydrophobicity

Fig. 5 shows sliding angle as a function of fluorination degree ( $f_t$ ) for needle-like “composite” surfaces of fluorocarbon coatings, on which the water–solid interface conditions of  $f_t^w = f_c^w = 0.5$  are realized. The results were obtained by using Eq. (5) in combination with Eqs. (1) and (4) for surfaces with  $R = 1.15$ , and a water droplet mass of 25 mg, in accordance with the surface model of Miwa et al. [33]. For simplicity, the constant  $k$  was chosen to be of  $13.9 \text{ mJ/m}^2$  and independent of F content of the coatings. This value was reported by Wolfram and Faust as the experimental constant for smooth Teflon [34]. It is believed that this value represents the interaction between water and highly fluorinated carbon coatings (mainly polymer-like fluorocarbons). It is clear that increasing

$f_t$  results in reduced water sliding angles, thus enhancing surface dynamic hydrophobicity.

Strictly speaking, being related to the solid–water interaction energy [33–35], the constant  $k$  should be  $f_t$  dependent. Representing the surface energy of a solid,  $k$  is expected to be slightly larger for coatings with low values of  $f_t$ , and lower for those with high  $f_t$ . Such an  $f_t$ -dependent value of  $k$  is believed to result in somewhat higher sliding angles at low  $f_t$ , thus indicating stronger solid–water interactions for low-F-containing coatings.

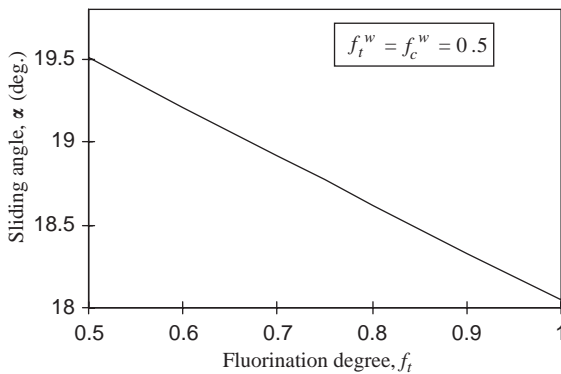


Fig. 5. Sliding angle of rough fluorocarbon “composite” surfaces as a function of their fluorination degree ( $f_t$ ) at surface water coverage ( $f_t^w = f_c^w$ ) equal to 0.5 calculated from Eq. (5). Water droplet mass is 25 mg.

Fig. 6a shows a relation between the sliding angle and area fractions of water coverage of fluorinated and “carbon-like” domains of “composite” needle-like surfaces. Because of the nanometer-scale character of two-phase heterogeneity, which can be expected for various fluorocarbon coatings, in Fig. 6b, similar to Fig. 5, we consider only the water coverage conditions with  $f_t^w = f_c^w$ ; three cases of the fluorinated degree  $f_t = 0.5$  (1), 0.7 (2), and 0.9 (3) are shown. From Fig. 6b, it can be concluded that lower water sliding angles may be attained on hydrophobic surfaces with low fractions of water coverage ( $f_t^w = f_c^w$ ) and higher fluorination degree ( $f_t$ ). Because of high air ratio at the water–solid interface, sliding resistance of such surfaces is reduced, leading to lower sliding angles.

Note that curves presented in Fig. 6b describe surface structures with same water-coverage parameters, which change along the abscissa, rather than with same geometrical topographies. Hence, when topologically equal needle-like substrates are coated with C–F materials with different  $F$  concentrations, water will tend to penetrate less between the needle-like posts with higher fluorination degree  $f_t$ . Thus, to keep the water-coverage parameters constant at higher values of  $F$  content, the topography of the substrate should be “adjusted”; in the simplest case of constant needle

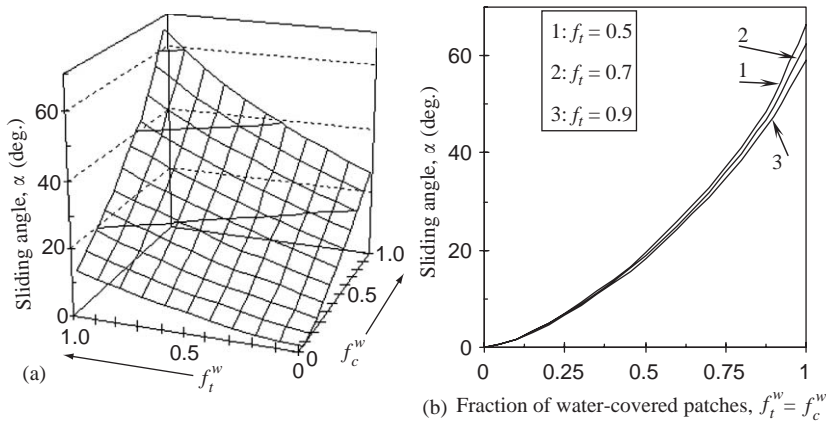


Fig. 6. (a) Sliding angle of rough fluorocarbon “composite” surfaces calculated from Eq. (5) as a function of water coverage of “teflon-like” patches ( $f_t^w$ ) and “carbon-like” patches ( $f_c^w$ ) at fluorination degree  $f_t = 0.5$ . (b) Sliding angle as a function of area fraction of surface water-covered patches ( $f_t^w = f_c^w$ ) for surfaces with different fluorination degree:  $f_t = 0.5$  (1), 0.7 (2), and 0.9 (3). Water droplet mass is 25 mg.

geometry and uniform needle-like structure, the distance between the needles should be increased, thus allowing water to penetrate deeper along the needles and satisfy the requirement of constant water–solid interface fraction ( $f_i^w = f_c^w = \text{constant}$ ). And vice versa, keeping the substrate topography constant, at increased fluorine content of coatings, one should expect a constant decrease in water coverage of the surface (lower  $f_i^w = f_c^w$ ). As a result, sliding behavior of water on such surfaces will be more  $f_i$  dependent, and the difference between the curves will be more significant than can be observed in Fig. 6b for any value of  $f_i^w = f_c^w$ . Thus, Fig. 6b is only a very qualitative approximation allowing, however, to reveal the character and tendencies of sliding behavior of “composite” fluorocarbon surfaces as a function of their water-coverage fraction.

It is also worth mentioning that the approach used in this study does not account for the geometry/topography of the surfaces under consideration. Thus far, there has been only limited research on how surface shapes and dimensions (roughness topography) influence static and/or dynamic hydrophobicity of rough surfaces [20,21,33]. The topography of the surface roughness, however, is extremely important in determining hydrophobicity; a proper interval and height difference in the microstructure are required to entrap air and thus provide both high contact angles and low sliding angles on rough hydrophobic surfaces [20,21,27,28,33]. Thus, additional research, combining both experimental and theoretical approaches, is required to further understand the effect of roughness topography on the wetting behavior of various fluorinated carbon surfaces.

#### 3.4. On snow and ice repellency of fluorocarbon coatings

Crucial in the icing-deicing problem is the ice/substrate interface, its chemistry and physics. It is commonly accepted that finding low-energy surfaces or coatings and introducing air between the ice and solid stand among the major strategies to reduce ice/surface adhesion that have previously been proposed in the literature [22,23,26–28]. As

coatings with low free surface energy, certain fluorocarbon coatings have already attracted attention of investigators in this field [12,13,22,25]. However, there is still a lack of systematic knowledge on snow and ice repellency of these materials. Taking the above into consideration, the following conclusions can be drawn.

- (1) Fluorinated carbon coatings with low F content are hardly expected to demonstrate attractive snow- and ice-repellent properties (as being hydrophilic). It is shown in the previous sections that only coatings with their fluorination degree over some certain value demonstrate hydrophobicity, the latter being enhanced with further increase in F concentration and air inclusion. This conclusion is supported by the report of Futama et al. [25] who improved hydrophobic properties of low-fluorine-containing coatings by additional treatment in silane solutions, since the as-deposited coatings contained insufficient amount of fluorine.
- (2) While searching for snow/ice-repellent coatings, one should keep in mind that very highly F-concentrated materials do not provide high hardness, being polymer-like materials [1,5,12–14]. Therefore, a compromise between extremely hard low-F-containing amorphous carbon coatings and hydrophobic polymer-like coatings with very high F concentration is likely to be found.
- (3) The use of rough fluorocarbon coatings, by deposition on patterned substrates or by forming rough coatings [3,9,16,19–21,32,33] seems to be also perspective. Such surfaces, if the requirement of proper interval and height difference in their microstructure is satisfied, can entrap air [19–22,32,33], thus reducing the solid–water interaction. This conclusion is consistent with the experimental results of Saito et al. [22], who reported a linear correlation between the contact angle of water and ice adhesion strength for rough “composite” water-repellent coatings of PTFE particles dispersed in polyvinylidene fluoride resin binder. Thus, properly designed/patterned

rough fluorocarbon coatings are also expected to be good candidates for ice-repellent applications.

#### 4. Summary and conclusions

Wetting characteristics of fluorocarbon coatings, as potential snow- and ice-repellent materials with low and controllable surface energy, are theoretically investigated in a wide range of both surface fluorination degree and surface roughness. Analysis is based on a simple model considering surface roughness and chemical heterogeneity to evaluate wettability of C–F coatings. Apparent contact angles of water on both smooth and rough (with air entrapped) fluorocarbon surfaces are modeled as functions of the fluorination degree and area fraction of air trapped into the water–solid interface. It is shown that C–F coatings with low fluorination degree are hardly hydrophobic and are not likely to provide snow or ice-repellent properties. At the same time, coatings with higher F concentration demonstrate good hydrophobicity, which can be further enhanced by air entrapment into rough surface structures. Thus, as coatings with good mechanical properties, low surface energy and surface roughness governed by deposition parameters or provided by proper substrates, such C–F materials, may be of potential use for snow- and ice-repellent purposes. Further investigations on fluorinated carbon coatings are required in order to link their real surface topography and chemistry with their water-repellent (and snow/ice-repellent) properties.

#### Acknowledgments

This work was carried out within the framework of the NSERC/Hydro-Quebec/UQAC Industrial Chair on Atmospheric Icing of Power Network Equipment (CIGELE) as well as the Canada Research Chair, tier 1, on Engineering of Power Network Atmospheric Icing (INGIVRE) at the University of Quebec in Chicoutimi. The authors would like to thank all the sponsors of the project.

#### References

- [1] Trojan K, Grischke M, Dimigen H. *Phys Stat Sol A* 1994;145:575–85.
- [2] Chua DHC, Teo KBK, Tsai TH, Milne WI, Sheeja D, Tay BK, Schneider D. *Appl Surf Sci* 2004;221:455–66.
- [3] Angleraud B, Tessier PY. *Surf Coat Technol* 2004;180/181:59–65.
- [4] Maia da Costa MEH, Baumvol IJR, Radke C, Jacobsohn LG, Zamora RRM, Freire FL. *J Vac Sci Technol A* 2004;22:2321–8.
- [5] Tang GZ, Ma XX, Sun MR, Li XD. *Carbon* 2005;43:345–50.
- [6] Kim JD, Sugimura H, Takai O. *Vacuum* 2002;66:379–83.
- [7] Yu GQ, Tay BK, Sun Z. *Surf Coat Technol* 2005;191:236–41.
- [8] Zhang P, Tay BK, Yu GQ, Lau SP, Fu YQ. *Diam Relat Mater* 2004;13:459–64.
- [9] Cao DM, Meng WJ, Simko SJ, Doll GL, Wang T, Kelly KW. *Thin Solid Films* 2003;429:46–54.
- [10] Chua DHC, Milne WI, Tay BK, Zhang P, Ding XZ. *J Vac Sci Technol A* 2003;21:353–8.
- [11] Butter RS, Waterman DR, Lettington AH, Ramos RT, Fordham EJ. *Thin Solid Films* 1997;311:107–13.
- [12] Ji H, Côté A, Koshel D, Terreault B, Abel G, Ducharme P, Ross G, Savoie S, Gagné M. *Thin Solid Films* 2002;405:104–8.
- [13] Koshel D, Ji H, Terreault B, Côté A, Ross GG, Abel G, Bolduc M. *Surf Coat Technol* 2003;173:161–71.
- [14] Yu GQ, Tay BK, Sun Z, Pan LK. *Appl Surf Sci* 2003;219:228–37.
- [15] Biloiu C, Biloiu IA, Sakai Y, Suda Y, Ohta A. *J Vac Sci Technol A* 2004;22:13–9.
- [16] Stelmashuk V, Biederman H, Slavínská D, Zemek J, Trchová M. *Vacuum* 2005;77:131–7.
- [17] Maréchal N, Pauleau Y. *J Vac Sci Technol A* 1992;10:477–83.
- [18] Quaranta F, Valentini A, Favia P, Lamendola R, d'Agostino R. *Appl Phys Lett* 1993;63:10–1.
- [19] Cicala G, Milella A, Palumbo F, Favia P, d'Agostino R. *Diam Relat Mater* 2003;12:2020–5.
- [20] Cheng YH, Chou CK, Chen C, Cheng SY. *Chem Phys Lett* 2004;397:17–20.
- [21] Gerbig YB, Phani AR, Haefke H. *Appl Surf Sci* 2005;242:251–5.
- [22] Saito H, Takai K, Yamauchi G. *Surf Coat Int* 1997;80:168–72.
- [23] Somlo B, Gupta V. *Mech Mater* 2001;33:471–80.
- [24] Kako T, Nakajima A, Irie H, Kato Z, Uematsu K, Watanabe T, Hashimoto K. *J Mater Sci* 2004;39:547–55.
- [25] Futamata M, Gai X, Itoh H. *Vacuum* 2004;73:519–25.
- [26] Putrenko VF, Peng S. *Can J Phys* 2003;81:387–93.
- [27] Kulinich SA, Farzaneh M. *Surf Sci* 2004;573:379–90.
- [28] Kulinich SA, Farzaneh M. *Appl Surf Sci* 2004;230:232–40.
- [29] Fowkes FM, Harkins WD. *J Am Chem Soc* 1940;62:3377–86.
- [30] Israelachvili JN, Gee ML. *Langmuir* 1989;5:288–9.

- [31] Wenzel RN. *Ind Eng Chem* 1936;28:988–94.
- [32] Nakajima A, Hashimoto K, Watanabe T. *Monatsh Chem* 2001;132:31–41.
- [33] Miwa M, Nakajima A, Fujishima A, Hashimoto K, Watanabe T. *Langmuir* 2000;16:5754–60.
- [34] Wolfram E, Faust R. Liquid drops on a tilted plate, contact angle hysteresis and the Young contact angle. In: Padday JF, editor. *Wetting, spreading and adhesion*. London: Academic Press; 1978. p. 213–22.
- [35] Murase H, Nanishi K, Kogure H, Fujibayashi T, Tamura K, Haruta N. *J Appl Polym Sci* 1994;54:2051–62.
- [36] Kiuru M, Alakoski E. *Mater Lett* 2004;58:2213–6.
- [37] Suzuki S, Nakajima A, Kameshima Y, Okada K. *Surf Sci* 2004;557:L163–8.